OPEN

Citation: Cell Death and Disease (2013) 4, e862; doi:10.1038/cddis.2013.387

www.nature.com/cddis

The inhibition of 2-arachidonoyl-glycerol (2-AG) biosynthesis, rather than enhancing striatal damage, protects striatal neurons from malonate-induced death: a potential role of cyclooxygenase-2-dependent metabolism of 2-AG

S Valdeolivas[1,2,3,5], MR Pazos[1,2,3,5], T Bisogno[4], F Piscitelli[4], FA Iannotti[4], M Allarà[4], O Sagredo*[,1,2,3,6], V Di Marzo*[,4,6] and J Fernández-Ruiz*[,1,2,3,6]

The cannabinoid CB_2 receptor, which is activated by the endocannabinoid 2-arachidonoyl-glycerol (2-AG), protects striatal neurons from apoptotic death caused by the local administration of malonate, a rat model of Huntington's disease (HD). In the present study, we investigated whether endocannabinoids provide tonic neuroprotection in this HD model, by examining the effect of O-3841, an inhibitor of diacylglycerol lipases, the enzymes that catalyse 2-AG biosynthesis, and JZL184 or OMDM169, two inhibitors of 2-AG inactivation by monoacylglycerol lipase (MAGL). The inhibitors were injected in rats with the striatum lesioned with malonate, and several biochemical and morphological parameters were measured in this brain area. Similar experiments were also conducted *in vitro* in cultured M-213 cells, which have the phenotypic characteristics of striatal neurons. O-3841 produced a significant reduction in the striatal levels of 2-AG in animals lesioned with malonate. However, surprisingly, the inhibitor attenuated malonate-induced GABA and BDNF deficiencies and the reduction in Nissl staining, as well as the increase in GFAP immunostaining. In contrast, JZL184 exacerbated malonate-induced striatal damage. Cyclooxygenase-2 (COX-2) was induced in the striatum 24 h after the lesion simultaneously with other pro-inflammatory responses. The COX-2-derived 2-AG metabolite, prostaglandin E_2 glyceryl ester (PGE_2-G), exacerbated neurotoxicity, and this effect was antagonized by the blockade of PGE_2-G action with AGN220675. In M-213 cells exposed to malonate, in which COX-2 was also upregulated, JZL184 worsened neurotoxicity, and this effect was attenuated by the COX-2 inhibitor celecoxib or AGN220675. OMDM169 also worsened neurotoxicity and produced measurable levels of PGE_2-G. In conclusion, the inhibition of 2-AG biosynthesis is neuroprotective in rats lesioned with malonate, possibly through the counteraction of the formation of pro-neuroinflammatory PGE_2-G, formed from COX-2-mediated oxygenation of 2-AG. Accordingly, MAGL inhibition or the administration of PGE_2-G aggravates the malonate toxicity.

Cell Death and Disease (2013) **4,** e862; doi:10.1038/cddis.2013.387; published online 17 October 2013
Subject Category: Neuroscience

Cannabinoids have been recently proposed as neuroprotecting agents in Huntington's disease (HD).[1–3] HD is an adult-onset and autosomal-dominant neurodegenerative disorder characterized by the progressive death of specific neuronal subpopulations within the striatum and the cerebral cortex.[4] HD is caused by a CAG triplet expansion in the gene coding the protein huntingtin,[5] which is toxic for these neuronal subpopulations, although the mechanism(s) responsible for this particular preference in neuronal degeneration in HD remains to be fully identified. An important challenge in HD is

[1]Departamento de Bioquímica y Biología Molecular, Instituto Universitario de Investigación en Neuroquímica (IUIN), Facultad de Medicina, Universidad Complutense, Madrid, Spain; [2]Centro de Investigación Biomédica en Red sobre Enfermedades Neurodegenerativas (CIBERNED), Madrid, Spain; [3]Instituto Ramón y Cajal de Investigación Sanitaria (IRYCIS), Madrid, Spain and [4]Endocannabinoid Research Group, Institute of Biomolecular Chemistry, Consiglio Nazionale delle Ricerche, Via Campi Flegrei 34, Comprensorio Olivetti, Pozzuoli, Naples, Italy
*Corresponding author: O Sagredo or J Fernández-Ruiz, Department of Biochemistry and Molecular Biology, Faculty of Medicine, Complutense University, 28040 Madrid, Spain. Tel: +34 91 3941450; Fax: +34 91 3941691; E-mails: onintza@med.ucm.es or jjfr@med.ucm.es or J.Fernandez-Ruiz@ciberned.es
or V Di Marzo, Endocannabinoid Research Group, Institute of Biomolecular Chemistry, Consiglio Nazionale delle Ricerche, Via Campi Flegrei 34, Comprensorio Olivetti, 80078 Pozzuoli, Naples, Italy. Tel: +39 081 8675093; Fax: +39 081 8041770; E-mail: vdimarzo@icmib.na.cnr.it
[5]These authors contributed equally to this work.
[6]These authors share senior authorship.
Keywords: endocannabinoids; CB1 and CB2 receptors; diacyl-glycerol lipase; monoacyl-glycerol lipase; cyclooxygenase-2; Huntington's disease; malonate; neuroprotection
Abbreviations: 2-AG, 2-arachidonoyl-glycerol; BDNF, brain-derived neurotrophic factor; COX-2, cyclooxygenase-2; DAGL, diacylglycerol lipase; DMSO, dimethylsulfoxide; GABA, γ-aminobutiric acid; GFAP, glial fibrillary acidic protein; HD, huntington's disease; HPLC, high-performance liquid chromatography; iNOS, inducible nitric oxide synthase; LC-APCI-MS, liquid chromatography/atmospheric pressure chemical ionization/mass spectrometry; LC-ESI-IT-ToF, liquid chromatography-electrospray-ion trap-time of flight; OEA, oleylethanolamide; OPA, o-phthaldehide; PBS, phosphate-buffered saline; PEA, palmitoylethanolamide; PGE_2-G, prostaglandin E_2-glycerol ester
Received 06.8.13; accepted 02.9.13; Edited by RA Knight

the development of efficient therapies to halt or slow down disease progression,[6,7] because the therapies investigated to date have been poorly effective. Compounds like minocycline, unsaturated fatty acids, coenzyme Q-10 and inhibitors of histone deacetylases are presently under clinical investigation,[8] whereas not only certain cannabinoid compounds, including both CB_1 and CB_2 receptor agonists, but also antioxidant phytocannabinoids have been successfully assayed in preclinical models[9–16] and have recently been applied in the clinical testing.[17]

The endocannabinoid system, which encompasses not only CB_1 and CB_2 receptors but also their endogenous ligands, the endocannabinoids anandamide and 2-arachidonoylglycerol (2-AG), and the enzymes for endocannabinoid biosynthesis and degradation, is subject to dysregulation in animal models of HD.[1,2,18] In particular, a strong correlation exists between reduced striatal levels of anandamide and 2-AG and locomotor signs of HD in R6/2 mice, genetic model of HD,[19] as well as in 3-nitropropionate-lesioned rats,[20] thus suggesting that impaired biosynthesis or exaggerated degradation of endocannabinoids might underlie in part the hyperkinesias typical of this disorder. Although this hypothesis was supported in part by the beneficial effect of inhibitors of endocannabinoid degradation,[21] it is not known whether the inhibition of endocannabinoid biosynthesis can worsen HD signs.

In the present study, we focused on striatal degeneration generated by the complex II inhibitor malonate, which is known to result in the death of striatal neurons through mechanisms that involve mainly the apoptotic machinery.[22] In this model, CB_2 receptor agonists protected striatal neurons from apoptotic death,[12] whereas the blockade of CB_1 receptors enhanced the magnitude of malonate-induced lesion.[23] Now, we wanted to determine the effects that the lesion with malonate produces on the striatal endocannabinoid levels. In particular, we expected that the inhibition of diacylglycerol lipases (DAGLs), the enzymes that catalyse the biosynthesis of 2-AG, with the compound O-3841,[24] would aggravate the effect of this lesion. However, on the basis of the initial unexpected finding of a neuroprotective effect of this inhibitor, our study progressed to additional objectives: (i) to elucidate what type of effect would be produced on the lesion by the opposite pharmacological manipulation, that is the blockade of the monoacylglycerol lipase (MAGL) and (ii) to investigate whether the biotransformation of 2-AG in prostaglandin glyceryl esters (PG-Gs) by cyclooxygenase-2 (COX-2) might explain the paradoxical effects found with O-3841, given that this type of oxygenated derivatives of 2-AG has been previously related to neurotoxic effects.[25] For these studies, we also used cultured M-213 cells, which share many phenotypic characteristics with striatal neurons.[26]

Results

Effects of DAGL inhibition on the striatal degeneration caused by malonate. The original objective of this study was to examine the effects of the DAGL inhibitor O-3841[27] on the striatal damage caused by malonate. As expected, the local administration of O-3841 produced a significant reduction in the striatal levels of 2-AG in animals lesioned with malonate ($F(2,17) = 4.111$, $P < 0.05$), without affecting the levels of anandamide (Figure 1a). Importantly, unlike other models of HD,[19,20] neither anandamide nor 2-AG was altered by the lesion of the striatum with malonate. Given the neuroprotective properties described for 2-AG,[28] a reduction in the levels of this endocannabinoid by O-3841 was expected to enhance the magnitude of malonate-induced lesion. However, our data indicate that the inhibitor enhanced the survival of striatal neurons as could be demonstrated by its capability to partially attenuate the malonate-induced deficit in GABA ($F(2,15) = 12.56$, $P < 0.01$; Figure 1b) and BDNF ($F(2,12) = 4.04$, $P < 0.05$; Figure 1c). It also enhanced the number of Nissl-stained neurons that had been markedly reduced by malonate ($F(2,18) = 26.46$, $P < 0.0001$; Figures 1d and e) and attenuated the glial activation caused by this neurotoxin, as indicated by the reduction in the intensity of immunostaining for the marker of astrocytes GFAP ($F(2,13) = 4.623$, $P < 0.05$; Figures 1f and g). Looking at the representative microphotographs of the three groups under investigation, it was evident that astrocytes underwent morphological alterations after the lesion, similar to those previously reported.[29] Such alterations were notably reduced by the treatment with O-3841 (Figure 1g).

Effects of malonate lesion on COX-2 and other pro-inflammatory responses and PGE_2-G formation. The above data contrast with the notion that 2-AG is neuroprotective, although a few studies demonstrated that, under certain circumstances, 2-AG may be also neurotoxic, in part through the generation of COX-2-derived metabolites.[25] We examined this possibility by analysing the effects of malonate on the expression of COX-2 as well as on the levels of one of the most representative COX-2 derivative of 2-AG, the PGE_2-G. We have also quantitated the expression of other mediators (e.g., iNOS, PPAR-α, PPAR-γ) that have been reported to have an instrumental role in proinflammatory events in neurodegenerative disorders.[30] Our experiments revealed that malonate lesion upregulated COX-2 in the striatum, although this effect was evident only 24-h after the lesion ($F(2,10) = 10.17$, $P < 0.01$; Figure 2a), and the same pattern was seen for iNOS ($F(2,11) = 12.46$, $P < 0.005$; Figure 2b). In agreement with these responses, we found a reduction in the expression of PPARs (only significant in the case of PPAR-α: $F(2,8) = 15.21$, $P < 0.005$, but showing a trend towards a decrease in the case of PPAR-γ: $F(2,9) = 1{,}503$, ns; see Figures 2c and d), the activation of which is known to inhibit the expression of these pro-inflammatory enzymes—an effect that has been related to a reduction in NFκB signalling.[31]

The increase in COX-2 expression by malonate might be in favour of an increased generation of COX-2-derived 2-AG metabolites. We tried to demonstrate such an increase by analysing the levels of PGE_2-G in the malonate-lesioned striatum, and, particularly, after the inhibition of MAGL, which should facilitate the formation of PGE_2-G (see below). Although our method, described here for the first time, was extremely sensitive (by allowing the quantification of as little as 50 fmols of PGE_2-G), we did not detect any PGE_2-G-like peak after LC-ESI-IT-ToF analysis. This, considering the average amount of striatal tissue that we analysed, indicates

a

Groups	AEA (pmol/g)	2-AG (nmol/g)
Control	54.9 ± 5.8	1.5 ± 0.2
+ malonate	53.7 ± 3.5	1.8 ± 0.2
+ malonate + O-3841	52.7 ± 11.9	1.1 ± 0.1*

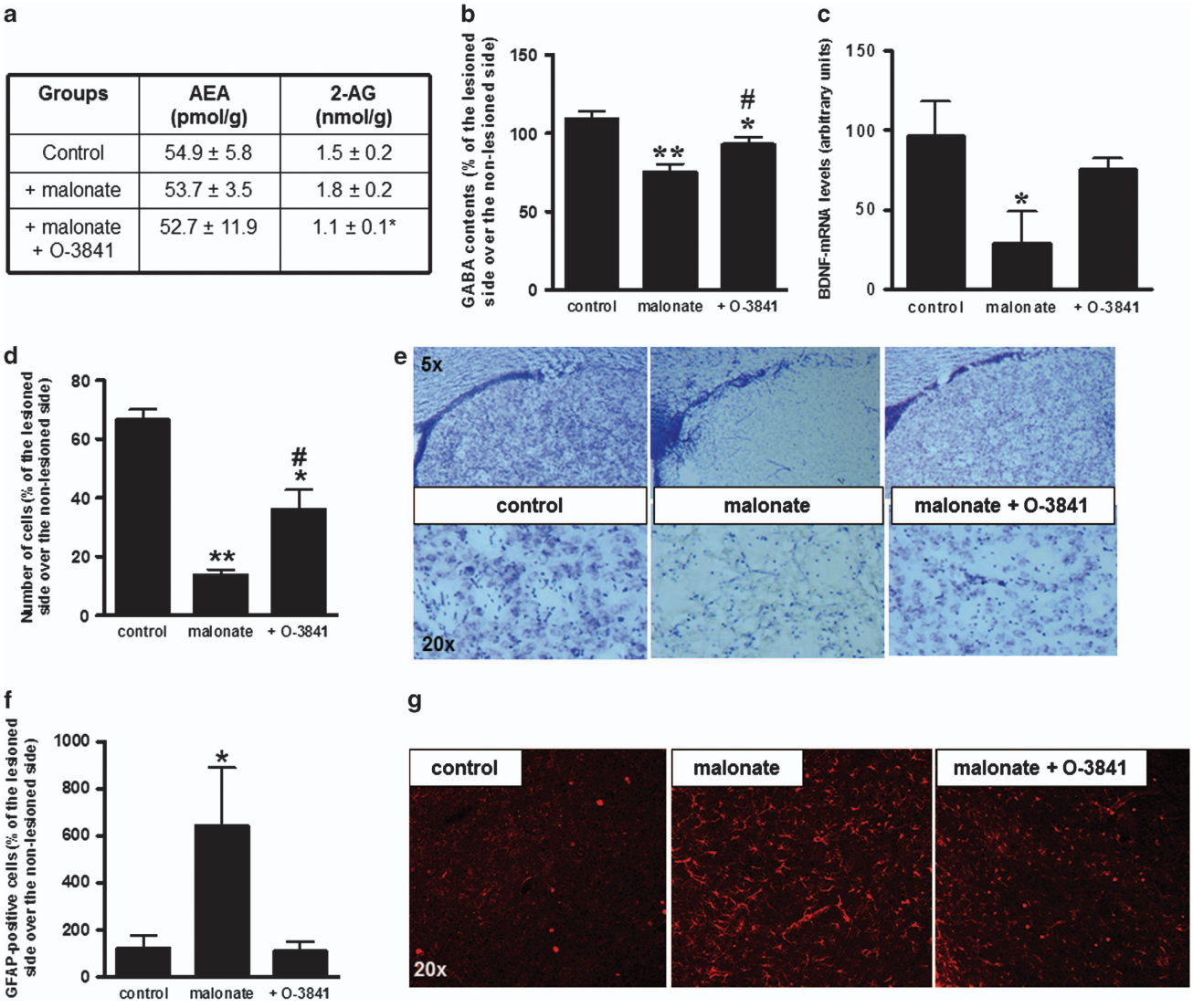

Figure 1 Levels of endocannabinoids (panel **a**), GABA (panel **b**), BDNF-mRNA (panel **c**), number of Nissl-stained cells (panel **d** and representative microphotographs in panel **e**) and GFAP immunostaining (panel **f** and representative microphotographs in panel **g**), measured in the striatum of malonate-lesioned rats after DAGL inhibition with O-3841 (250 ng administered locally) and of their sham-operated controls. See details in the text. Values are means ± S.E.M. of 5–7 animals *per* group. Data were assessed by one-way analysis of variance followed by the Student–Newman–Keuls test (*$P<0.05$, **$P<0.005$ *versus* controls; $^{\#}P<0.05$ *versus* the group treated with malonate)

that less than 1.9 pmol/g wet tissue weight of PGE_2-G are present in the striatum of malonate-treated rats. However, this finding does not necessarily imply that PGE_2-G was not formed under our experimental conditions, as the generation of this compound might be restricted only to those striatal areas where the lesion is more intense, and hence impossible to detect when the whole striatum is analysed.

Effects of MAGL inhibition on striatal degeneration caused by malonate. Next, we investigated whether the increase in 2-AG levels after MAGL inhibition would produce the opposite effect to the protection found with DAGL inhibition. We first worked with the non-covalent MAGL inhibitor OMDM169,[32] but the local administration of this compound did not produce any significant change in the levels of 2-AG and anandamide (Figure 3a), and it did not aggravate the effects of malonate on the striatal parenchyma measured by Nissl staining (Figure 3b). Therefore, we used the more potent MAGL inhibitor JZL184, which, compared with OMDM169, is covalent and also more selective and elicits an eightfold increase in 2-AG levels.[33] The Nissl staining in the striatal parenchyma revealed some apparent reduction in the number of stained cells that did not reach statistical significance (see Figure 3d), but the differences were evident and statistically significant in the case of GFAP immunostaining, which was higher in the malonate-lesioned animals treated with JZL184 ($F(2,10)=41.22$, $P<0.0001$; Figure 3c), thus indicating stronger astrogliosis in the striatal parenchyma of these animals. We assumed that this aggravating effect was caused by the biotransformation of 2-AG in PG-Gs despite the fact that, also in this case, we were unable to detect *in vivo* generation of PGE_2-G. To further explore this possibility, we decided to inject this 2-AG derivative directly into the striatum of malonate-lesioned rats

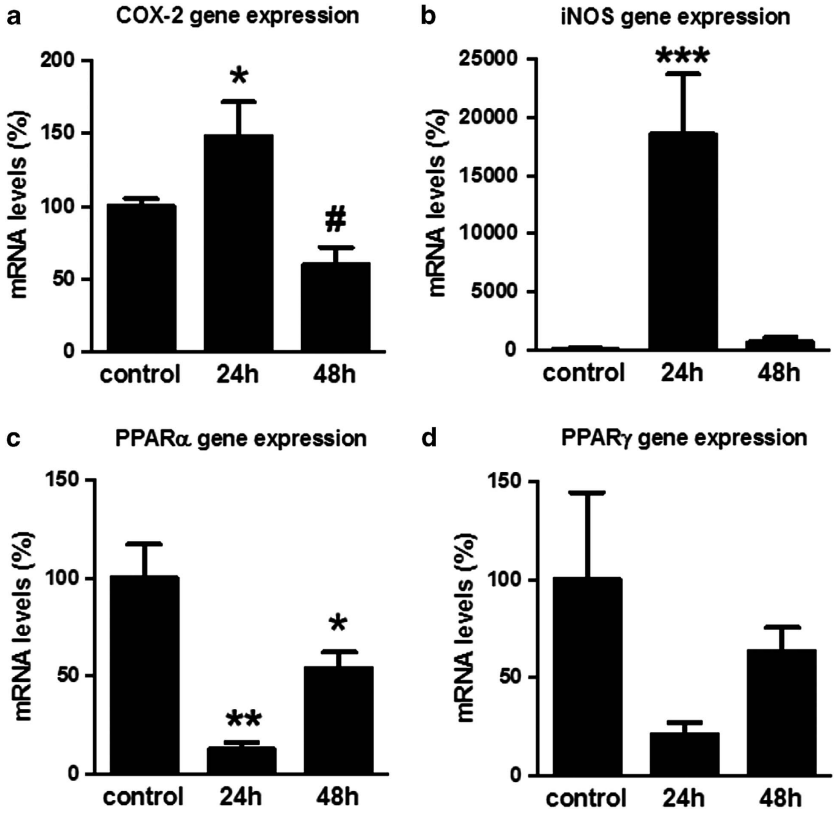

Figure 2 mRNA levels for COX-2 (**a**), iNOS (**b**), PPAR-α (**c**) and PPAR-γ (**d**) measured in the striatum of malonate-lesioned rats (at 24 or 48 hour after the injection) and of their sham-operated controls. See details in the text. Values are presented as means ± S.E.M. of 4–6 animals per group. Data were assessed by one-way analysis of variance followed by the Student–Newman–Keuls test ($^{*}P<0.05$, $^{**}P<0.005$, $^{***}P<0.0005$ *versus* the other groups; $^{\#}P<0.05$ *versus* the group treated with malonate)

and found a further reduction in the number of Nissl-stained cells in the striatal parenchyma that were partially attenuated by the co-administration of the PGE2-G antagonist AGN220675 ($F(3,15)=28.48$, $0<0.0001$; Figure 3e).

Induction of COX-2 in response to malonate and effects of MAGL inhibition in cultured M-213 cells. Given the difficulties to detect *in vivo* generation of PG-Gs in malonate-lesioned rats, we moved to an *in vitro* strategy using a cell line, M-213, which recapitulates some phenotypic characteristics of striatal neurons.[26] These cells were sensitive to malonate, which reduced the number of surviving cells by more than 50% at 6 h after the addition of the neurotoxin (Figure 4a). This was paralleled by a marked upregulatory response (>6 fold) in the expression of COX-2 (Figure 4b), reproducing the same response found *in vivo*, whereas the exposure to malonate downregulated the expression of MAGL and FAAH (Figures 4d and f). Accordingly, the activities of 2-AG and anandamide-hydrolysing enzymes, which in neurons are mostly accounted for MAGL and FAAH, respectively, were reduced (Figure 4c), and the same happened with the MAGL and FAAH levels (Figures 4e and g). Malonate did not affect the levels of anandamide and related *N*-acylethanolamines in these cells, whereas there was a trend towards an increase in the levels of 2-AG, although we were still unable to detect any significant change in the levels of PGE_2-G (Figure 4c). However, the addition of the MAGL inhibitor OMDM169 to the culture media tended to reduce the levels of 2-AG (Figure 5a) and allowed to detect for the first time PGE_2-G levels ($F(2,8)=17.22$, $P<0.005$; Figure 5b), precisely in the experimental condition in which the generation of this 2-AG derivative should be maximal. In agreement with this, we found an increase in malonate-induced cell death when 2-AG levels were elevated with OMDM169 ($F(2,14)=243.5$, $P<0.0001$; Figure 5c) and a trend towards an increase when we used JZL184 (Figure 5d). We also found that the addition of 2-AG *per se* enhanced malonate-induced cell death ($F(2,15)=130.6$, $P<0.0001$; Figure 5e). We conducted a pilot concentration–response study (0.1–50 μM), which showed that doses $<25\,\mu$M did not enhance malonate-induced cell death, whereas a significant potentiating effect was found with 25 and 50 μM (data not shown).

We next investigated whether the enhancing effect of MAGL inhibitors on malonate-induced cell death may be attenuated by the blockade with the PGE_2-G antagonist AGN220675 or by inhibiting COX-2 with celecoxib, which would provide further evidence of the role of 2-AG biotransformation in the effects investigated in this study. We used for these experiments the MAGL inhibitor JZL184, which produced a slight increase in malonate-induced cell death, and we found that both AGN220675 ($F(3,30)=8.605$, $P<0.005$; Figure 6a) and celecoxib ($F(3,21)=30.04$, $P<0.0001$; Figure 6b; we used two concentrations, 12.5 and 25 μM, both

a

Groups	AEA (nmol/g of lipid extract)	2-AG (nmol/g of lipid extract)
Control	2.3 ± 0.4	461.9 ± 60.0
+ malonate	2.3 ± 0.2	576.2 ± 31.1
+ malonate + OMDM169	1.9 ± 0.3	541.6 ± 78.1

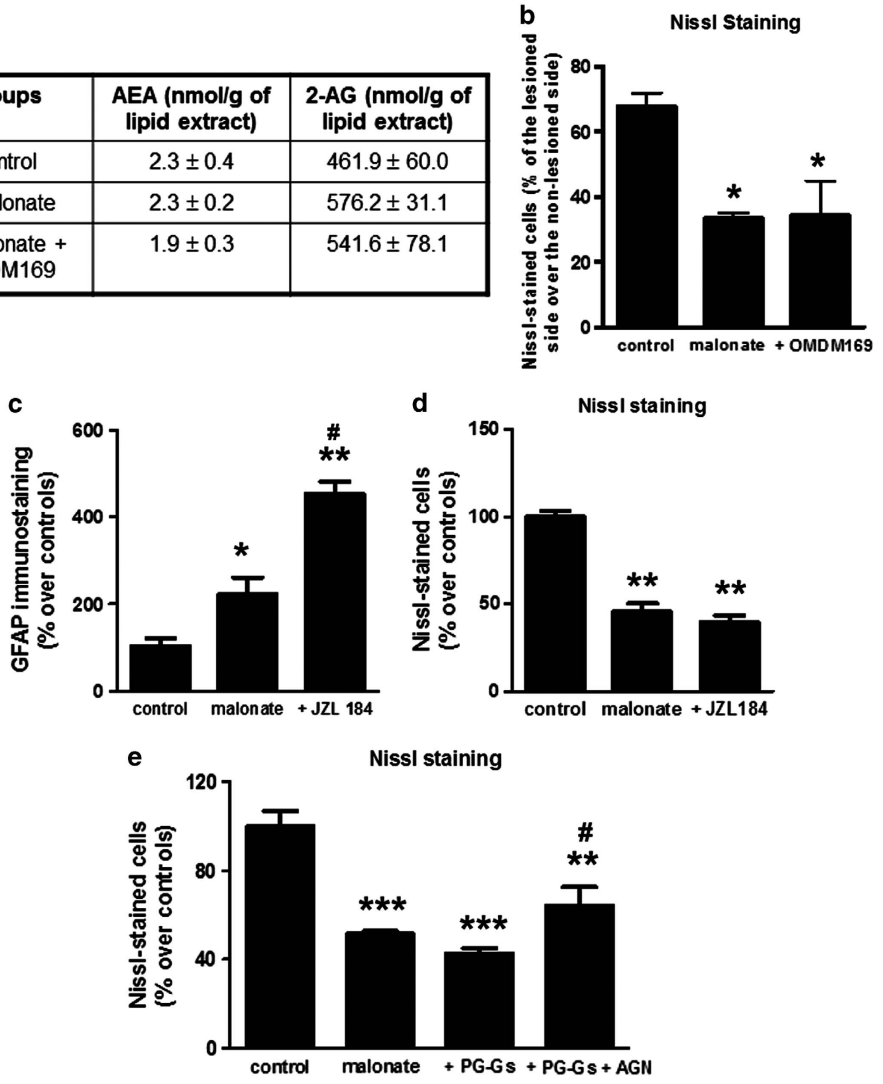

Figure 3 Amounts of endocannabinoids (panel **a**), number of Nissl-stained cells (panels **b**, **d** and **e**) and GFAP immunostaining (panel **c**), measured in the striatum of malonate-lesioned rats after MAGL inhibition with OMDM169 (500 ng administered locally) or JZL184 (4 mg/kg weight administered i.p.), or after the administration of PGE_2-G (10 μg administered locally) and/or AGN220675 (300 ng administered locally), and of their sham-operated controls. See details in the text. Values are means ± S.E.M. of 4–6 animals *per* group. Data were assessed by one-way analysis of variance followed by the Student–Newman–Keuls test (*$P<0.05$, **$P<0.001$, ***$P<0.005$ *versus* controls; #$P<0.05$ *versus* the group treated with malonate and PGE_2-G)

equally effective) reduced cell death compared with the effect found with the combination of malonate and JZL184. We next tried to obtain a similar result with the direct addition of 2-AG. We again found that 2-AG was able to enhance malonate-induced cell death ($F(4,29)=36.42$, $P<0.0001$; Figure 6c), but this response was not altered by the celecoxib-induced inhibition of COX-2 or by the PGE_2-G antagonist AGN220675 (Figure 6c), used at the same concentrations as in the experiments with JZL184. In addition, higher concentrations of AGN220675 (1 and 50 mM) were ineffective in this case (data not shown). This latter finding may be related to the rapid degradation of 2-AG to arachidonic acid and glycerol in absence of MAGL inhibition, and the subsequent generation of prostaglandins, rather than PG-Gs, by the action of COX-1 and, to a smaller extent, COX-2, which would explain the highest cell death found after the combination of 2-AG and malonate compared with the cells exposed to malonate alone (Figure 6c). In fact, this is supported by the observation that the incubation of these cells with 2-AG at the same concentration (25 μM) as in the above experiment, and also at a higher concentration (50 μM), but in absence of malonate, increased cell death (more than twofold for 25 μM 2-AG and almost fourfold for 50 μM 2-AG), and both responses were significantly enhanced by celecoxib ($F(4,31)=26.6$, $P<0.0001$; Figure 6d). This inhibitor might have blocked the formation of PGE_2-Gs by COX-2 acting on exogenous 2-AG and enhanced the amount of 2-AG available for arachidonic acid generation and the action of COX-1, with a subsequent greater generation of prostaglandins, which would cause cell death. Indeed, 2-AG hydrolysis is an important source of arachidonic acid and neuroinflammatory prostaglandins,[34] such that genetic or pharmacological inactivation of 2-AG hydrolysis provides beneficial effects in experimental Parkinsonism[34] and Alzheimer's disease.[35]

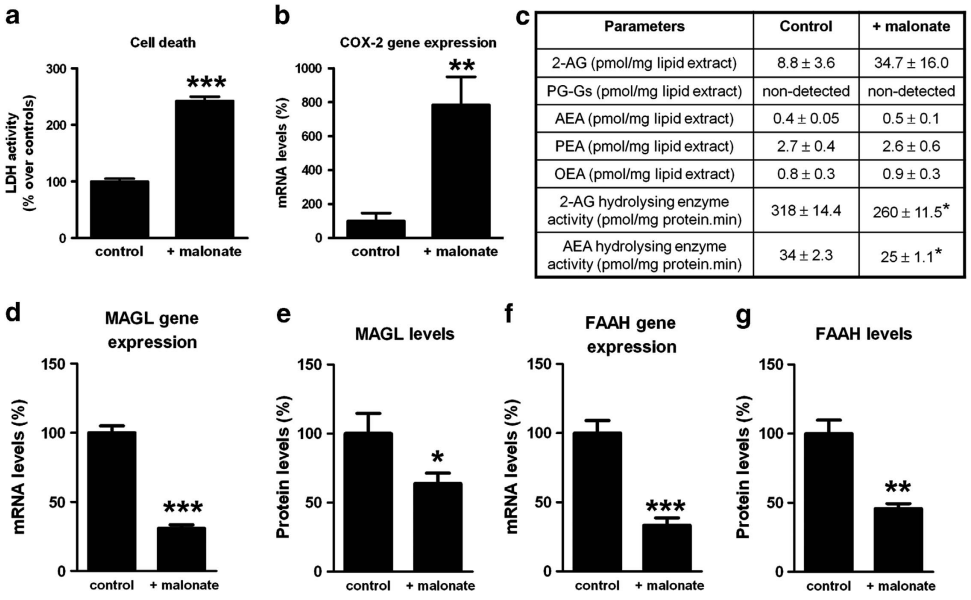

Parameters	Control	+ malonate
2-AG (pmol/mg lipid extract)	8.8 ± 3.6	34.7 ± 16.0
PG-Gs (pmol/mg lipid extract)	non-detected	non-detected
AEA (pmol/mg lipid extract)	0.4 ± 0.05	0.5 ± 0.1
PEA (pmol/mg lipid extract)	2.7 ± 0.4	2.6 ± 0.6
OEA (pmol/mg lipid extract)	0.8 ± 0.3	0.9 ± 0.3
2-AG hydrolysing enzyme activity (pmol/mg protein.min)	318 ± 14.4	260 ± 11.5*
AEA hydrolysing enzyme activity (pmol/mg protein.min)	34 ± 2.3	25 ± 1.1*

Figure 4 LDH activity (panel **a**), mRNA levels for COX-2 (panel **b**), MAGL (panel **d**) and FAAH (panel **f**), protein levels of MAGL (panel **e**) and FAAH (panel **g**) and levels of 2-AG, PGE2-G, anandamide and related *N*-acylethanolamines and activities of 2-AG- and anandamide-hydrolysing enzymes (panel **c**), measured in cultured M-213 cells treated for 6 h with 40 mM malonate. See details in the text. Values are presented as means ± S.E.M. of 5–7 cases per group (except in the measures of enzyme activities and protein levels that were three cases per group). Data were assessed by the unpaired Student's *t*-test (*$P<0.05$, **$P<0.01$, ***$P<0.005$ *versus* controls)

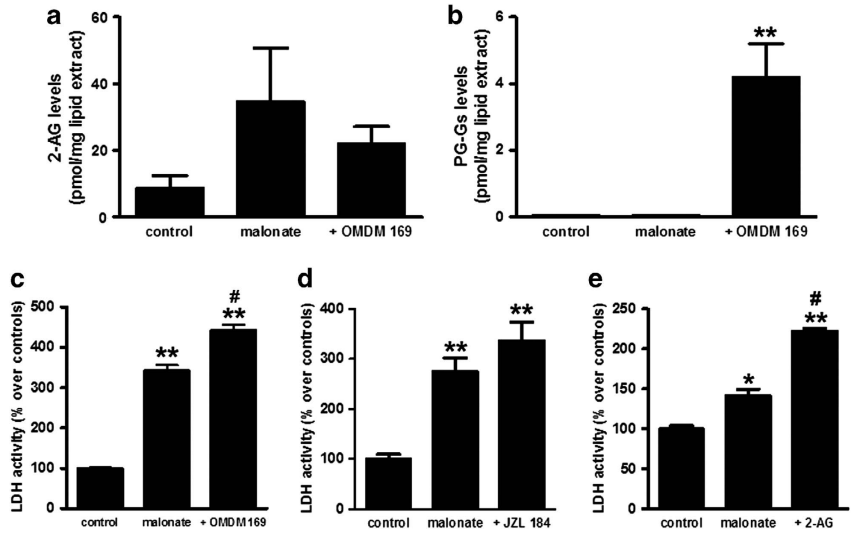

Figure 5 Amounts of 2-AG (panel **a**) and PGE_2-G (panel **b**), and LDH activity, measured in cultured M-213 cells treated for 6 h with 40 mM malonate and/or the inhibitors of MAGL, OMDM169, at 1 μM (panel **c**) or JZL184 at 10 nM (panel **d**), or with 40 nM malonate and/or 2-AG at 25 μM (panel **e**). See details in the text. Values are presented as means ± S.E.M. of 4–6 cases *per* group. Data were assessed by the one-way analysis of variance followed by the Student–Newman–Keuls test (*$P<0.05$, **$P<0.005$ *versus* controls; $^{\#}P<0.05$ *versus* malonate)

Discussion

Previous studies have shown that CB_2 receptor-deficient mice exhibit a greater sensitivity to malonate,[12] whereas the blockade of CB_1 receptors with rimonabant also enhanced the magnitude of striatal degeneration caused by this neurotoxin in rats.[23] In this context, we predicted that the blockade of 2-AG biosynthesis with the recently developed DAGL inhibitor O-3841[27] should also result in a greater sensitivity to malonate, given the previously reported neuroprotective effects of 2-AG through its capability to activate both cannabinoid receptors with similar efficacy.[28] Surprisingly, however, the administration of O-3841 to malonate-lesioned rats, rather than aggravating the striatal lesion, was accompanied by greater survival of striatal neurons and by the attenuation of glial activation typically associated with the malonate lesion.[12]

These unexpected observations found some support in recent studies that have demonstrated that 2-AG may also behave as a neurotoxic factor under special circumstances,

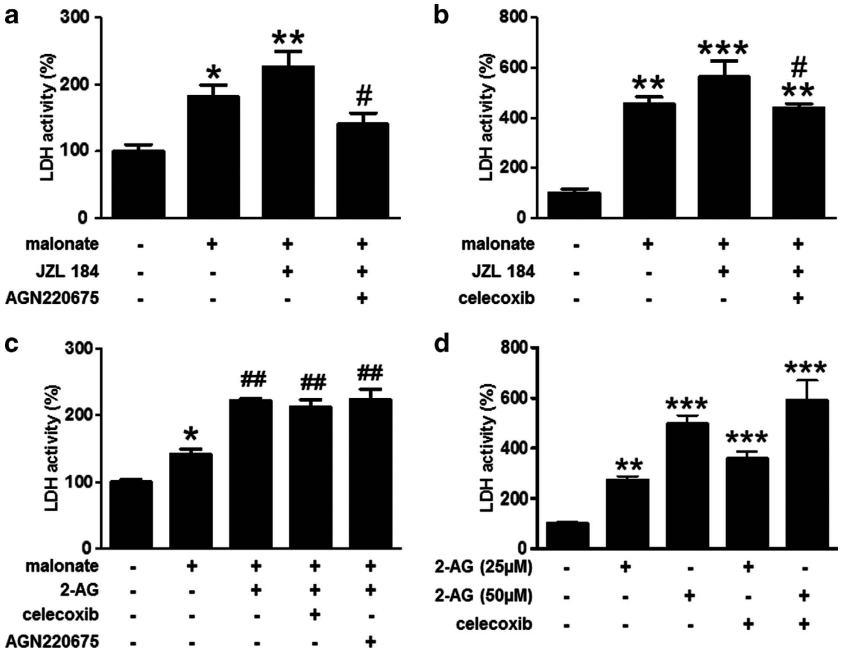

Figure 6 LDH activity measured in cultured M-213 cells treated for 6 h with 40 mM malonate and/or the inhibitor of MAGL JZL184 at 10 nM in the presence or absence of PGE_2-G antagonist AGN220675 at 25 μM (panel **a**) or the COX-2 inhibitor celecoxib at 12.5 μM (panel **b**), or with 40 nM malonate and/or 2-AG at 25 μM combined with celecoxib at 12.5 μM or AGN220675 at 25 μM (panel **c**), or treated directly with 2-AG at 25 or 50 μM and/or celecoxib at 12.5 μM (panel **d**). See details in the text. Values are presented as means ± S.E.M. of 6-8 cases *per* group. Data were assessed by the one-way analysis of variance followed by the Student–Newman–Keuls test ($^{*}P<0.05$, $^{**}P<0.005$, $^{***}P<0.0005$ *versus* controls; $^{\#}P<0.05$ *versus* malonate + JZL184; $^{\#\#}P<0.005$ *versus* malonate)

namely, during the overexpression of COX-2, a key response in neuroinflammatory events accompany neurodegeneration.[36–38] Thus, Sang *et al.*[25] reported that 2-AG may be a natural substrate of inducible COX-2 enzyme and generate a series of metabolites, known as PG-Gs,[39] the most abundant of which, PGE_2-G, is known to induce excitotoxic damage[25] and to exert pro-inflammatory and hyperalgesic effects.[40] In fact, 2-AG is oxygenated by COX-2 as effectively as arachidonic acid,[25] whereas the oxygenation of anandamide by this enzyme is slower.[41] Therefore, it appears that the key condition for the activation of this metabolic pathway would be that COX-2 enzyme is abnormally upregulated in response to a brain insult. In such situation, there would be an imbalance between the previously reported neuroprotective effects of 2-AG (mediated by the activation of either CB_1, CB_2 or other cannabinoid-related receptors;[28,42–44]) and its transformation by COX-2, which would generate potential neurotoxic metabolites like PGE_2-G. Our data support the existence of this imbalance in our experimental conditions, because we found an elevated COX-2 gene expression in the malonate-lesioned striatum compared with controls. We also found a similar early upregulatory response in other pro-inflammatory enzyme such as iNOS, which frequently accompanies COX-2 elevation.[30] In addition, we observed the expected down-regulation of PPAR-α and PPAR-γ, for which certain cannabinoids, including 2-AG (see below), have been recently found to act as agonists.[43,45] This may explain the observed increases in COX-2 and iNOS with the reduction of the PPAR-dependent inhibitory effect on NFκB signalling, which in turn is involved in the stimulation of the expression of these pro-inflammatory enzymes.[31] It is important to remark that the elevation of COX-2 has been already found in neurodegenerative disorders including HD,[36,46–48] having an instrumental role in the pathogenesis,[38] so that its reduction through different strategies (e.g., pharmacological inhibition) may reduce brain damage.[49] Interestingly, 2-AG may represent an important source of arachidonic acid and neuroinflammatory prostanoids in some of these disorders,[34,35] and, therefore, the neuroprotective and anti-inflammatory actions of O-3841 effect could be also explained by the interference with this mechanism. However, although in the studies in which 2-AG was shown to act as a biosynthetic precursor of neuroinflammatory prostanoids, MAGL inhibitors produced neuroprotective and anti-inflammatory effects,[34,35] here we found that MAGL inhibition results in a greater striatal damage both *in vivo* and *in vitro*. Therefore, our findings with O-3841 and JZL184/OMDM169 can only be interpreted by the interference with, or enhancement of, the generation of oxygenated derivatives of 2-AG by elevated activity of COX-2 (see Figure 7 panels A and B, respectively). In other words, the inhibition of DAGL might re-establish the balance between the neuroprotective and neurotoxic mechanisms of 2-AG, whereas the inhibition of MAGL would enhance this imbalance, which is, in fact, likely to be facilitated under conditions of reduced expression of this enzyme, as in the present case (see below).

On these premises, the next objective of our study became the demonstration that PG-Gs, in particular PGE_2-G, are generated in the striatum in response to malonate, and that they are reduced by DAGL inhibition and increased after MAGL inhibition. However, we were unable to find detectable levels of PGE_2-G after these manipulations *in vivo*, in

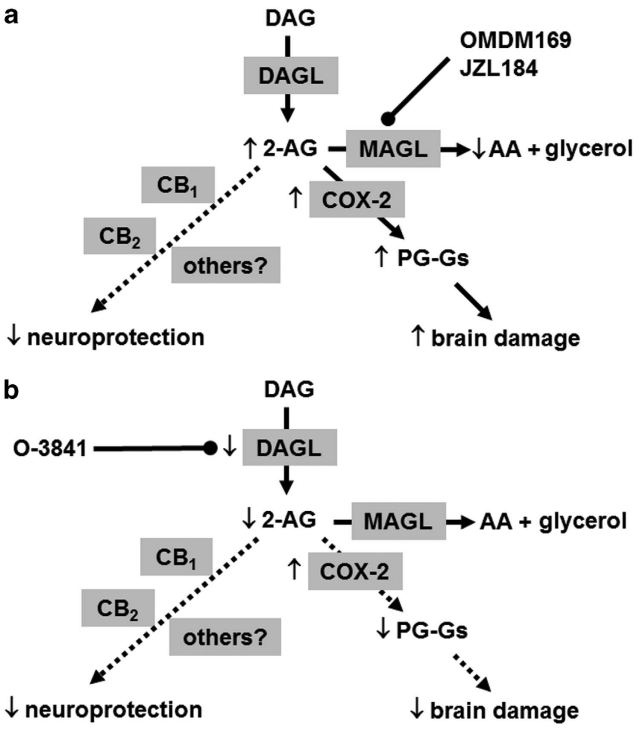

Figure 7 Schematic overview of possible mechanisms explaining the effect of 2-AG following malonate lesion and after MAGL (panel **a**) or DAGL (panel **b**) inhibition

particular after the lesion with malonate combined with MAGL inhibition, that is, the experimental conditions in which the generation of these derivatives would be maximal. On the basis of the detection limit of our analytical method, we estimated that an amount of less than 1.9 pmol/g wet tissue weight of this compound is present in the whole striatum from both unlesioned and lesioned rats, in agreement with previous findings indicating that the tissue concentrations of this compound, for example, in the rat paw, are in the order of the fmol/g wet tissue weight.[40] It is possible that the generation of this metabolite is restricted to the lesioned cells within the striatum, then rendering impossible its detection when the whole striatum needs to be used for biochemical determinations (see Results section).

Given the difficulties to detect the generation of PG-Gs from 2-AG in our *in vivo* model, we considered the possibility that pathways other than COX-2 metabolism of 2-AG may be involved in the generation of putative pro-inflammatory 2-AG-derived compounds, or that the neuroprotection shown by O-3841 was due to its interaction with targets other than DAGL. An attractive possibility would be the expected increase in the DAG levels derived from the inhibition of DAGL, as DAG signalling has been associated with cell proliferation, differentiation and survival/death decision.[50] However, our next experiments provided further evidence in support of a mechanism involving the generation of PG-Gs from 2-AG by the action of COX-2. First, we administered synthetic PGE_2-G to malonate-lesioned rats and found an aggravation of striatal damage that was partially reversed by the PGE_2-G antagonist AGN220675. Secondly, in experiments conducted *in vitro* with cultured M-213 cells, which also experience a marked upregulation of COX-2 in response to malonate, we showed that the increase in endogenous 2-AG levels derived from MAGL inhibition results in a greater cell death. This effect appeared to be related to the generation of PG-Gs as it was reversed by pharmacological manipulations that either inhibit the formation (e.g., inhibition of COX-2 with celecoxib) or block the action at its target(s) (e.g., AGN220675) of PGE_2-G. Indeed, the only experimental condition in which we were able to detect PGE_2-G was in these cells after the incubation with malonate combined with the MAGL inhibitor OMDM169, that is, the same experimental conditions in which cell death was maximal. Notably, malonate treatment of M-213 cells was accompanied by the downregulation of MAGL mRNA, protein and enzymatic activity, that is, another condition that, together with COX-2 upregulation, is expected to favour the formation of PG-Gs.

Another issue arising from our data and deserving some comments is the role that 2-AG may have in the upregulation of COX-2 observed here. A recent study[51] showed that COX-2 upregulation may be elicited by a loss in the endogenous inhibition of this enzyme exerted by 2-AG via CB_1 receptors. This was found in the hippocampus under pro-inflammatory and excitotoxic stimuli both *in vivo* and *in vitro*,[51] thus supporting the idea that neuroprotection exerted by 2-AG through the activation of CB_1 receptors might be used also to prevent the COX-2 elevation typical of several neuroinflammatory/neurodegenerative conditions. *A priori*, this possibility would be in contrast with our present hypothesis of 2-AG exerting a neurotoxic, rather than neuroprotective, effect. It is possible that neuroprotection with 2-AG is the predominant response when the levels of 2-AG are strongly elevated by the neurotoxic stimuli, as in the case of traumatic brain injury,[44] as this elevation would allow to prevent, among others, the upregulation of COX-2. In contrast, in our present case, in which 2-AG levels remained unaffected by the malonate-induced lesion, this might have allowed the upregulation of COX-2 and the subsequent potential transformation of basal 2-AG levels into PG-Gs by the action of this enzyme, thus supporting the above-mentioned idea of an imbalance between the neuroprotective and neurotoxic effects of 2-AG. Interestingly, a follow-up study by the same group[52] revealed that the inhibitory effect by 2-AG of COX-2 expression also involves the activation of PPAR-γ, for which we have found, under our experimental conditions, a trend towards downregulation. This downregulation effect might counteract the inhibition by 2-AG of COX-2, participate in COX-2 upregulation and facilitate the conversion by this enzyme of 2-AG in PG-Gs. It is also important to remark that the downregulation of PPARs observed in the malonate-lesioned rats would be another factor, in addition to elevated levels of COX-2, aggravating the imbalance between the neuroprotective and neurotoxic effects of 2-AG, as these nuclear receptors have been involved in part of the neuroprotective actions of 2-AG,[43,45] which would then be lost in malonate-lesioned rats.

In summary, the inhibition of 2-AG biosynthesis is accompanied by neuroprotection in rats lesioned with malonate. This effect seems to be related to a potential inhibition of certain pro-neuroinflammatory actions of 2-AG, particularly those involving its transformation into oxygenated metabolites by COX-2, an enzyme that was found here to be elevated in

the striatum after the lesion with malonate. In contrast, MAGL inhibition or the administration of PGE_2-G *in vivo* aggravated the malonate toxicity, and these effects were reproduced in cultured M-213 cells in which upregulation of COX-2 was also elicited by malonate.

Materials and methods

Animals, treatments and sampling. Male Sprague–Dawley rats were housed in a room with controlled photoperiod (08 : 00–20 : 00 light) and temperature ($22 \pm 1\,^{\circ}C$). They had free access to standard food and water and were used at an adult age (3-month old; 300–350 *g* weight) for experimental purposes, all conducted in an attempt to minimize animal pain and discomfort, and following local and European rules (directive 86/609/EEC). Rats were injected stereotaxically (coordinates: $+0.8$ mm anterior, $+2.9$ mm lateral from the bregma, -4.5 mm ventral from the dura mater) into the left striatum with 2 M malonate (dissolved in PBS 0.1 M, pH = 7.4) in a volume of 1 μl or were sham operated in the same left striatum but with no injection of the toxin. The contralateral striatum of each animal always remained unaffected, allowing analyses performed in this animal model lead to data frequently expressed as percentage of the lesioned side over the corresponding non-lesioned side. Animals were used for these experimental analyses 48 h later, except in the case of the time–course analysis of gene expression for COX-2, inducible nitric oxide synthase (iNOS) and peroxisome-proliferator activated receptors (PPAR) for which animals were sacrificed at 24 and 48 h after the lesion.

O-3841 (octadec-9-enoic acid 1-methoxymethyl-2-(fluoromethyl-phosphinoyloxy)-ethyl ester), a kind gift by Dr. A Mahadevan, Organix, Woburn, Massachussets, was synthesized as previously described.[27] The compound was dissolved in dimethylsulfoxide (DMSO) and diluted in 0.1 M PBS (pH = 7.4) for administration (final concentration of DMSO < 1%). As this compound is not expected to cross the blood–brain barrier, it was locally administered 30 min before the administration of malonate. Each animal received a unique administration of 250 ng of O-3841 in a volume of 1 μl. In additional experiments, 500 ng of OMDM169, synthesized as previously described,[32] 10 μg of prostaglandin E_2-glycerol ester (PGE_2-G; purchased from Cayman Chemical, Ann Arbor, Michigan, USA) and 300 ng of AGN220675 (generously provided by Dr. Woodward, Allergan, Irvine, CA, USA), prepared in 5% DMSO-saline, were also administered following the same procedure as in the case of O-3841. In another experiment, JZL184 (purchased from Tocris Bioscience, Bristol, UK, and dissolved in DMSO-Tween 80-saline, 1 : 1 : 18) was administered to malonate-lesioned rats at the dose of 4 mg/kg weight in two injections, 30 min before and 2 h after the intrastriatal injection of malonate, following our previously published procedure.[12] Malonate-lesioned animals, administered with the corresponding vehicle for all treatments (malonate group), as well as sham-operated animals (control group), were always included for each pharmacological experiment.

Depending on the experiment, animals were killed 24–48 h after the administration of malonate, and their brains were rapidly removed and frozen in 2-methylbutane, cooled in dry ice and stored until evaluation of neurochemical parameters indicating the degree of malonate-induced striatal injury. Some animals from each experimental group were perfused with 10% formalin, and their brains were post fixed during 3 h, cryoprotected and stored at $-20\,^{\circ}C$ before being sliced in a vibratome. This material was used for histological analyses. In a separate group of animals (only in the experiments with the DAGL inhibitor O-3841 or the MAGL inhibitor OMDM169), brains were dissected before freezing and their striata were weighed, frozen on dry ice and stored in eppendorf tubes at $-80\,^{\circ}C$ until lipid extraction and analysis of endocannabinoids and related compounds (PGE_2-G or *N*-acylethanolamines). The entire procedure took less than 5 min, which is significantly less than the amount of time required for postmortem generation of 2-AG, arachidonoylethanolamide (anandamide) or related compounds. Finally, in another separate experiment, malonate-injected and sham-operated rats were decapitated twice after the formation of the lesion (24 and 48 h). Their brains were quickly and carefully removed, the striata dissected and frozen for qRT-PCR analysis.

Cell culture. M-213-2O cells were a generous gift from Dr. WJ Freed (National Institute on Drug Abuse, Bethesda, MD, USA; see 26). Cells were maintained in Dulbecco's modified Eagle's medium (DMEM) supplemented with 10% fetal bovine serum, 2 mM ultra-glutamine, 1% non-essential amino acids and 1% penicillin/streptomycin (LONZA, Verviers, Belgium) and under a humidified 5% CO_2 atmosphere at $37\,^{\circ}C$. For cytotoxicity experiments, cells were seeded at 50000 cells/cm^2 in 24-well plates and maintained under a humidified atmosphere (5% CO2) at $37\,^{\circ}C$ overnight. Afterwards, normal medium was replaced by serum-free medium and cells were exposed to either OMDM169 (1 μM), JZL184 (10 nM), 2-AG (25 and 50 μM; purchased from Tocris Bioscience, Bristol, UK), celecoxib (12.5 or 25 μM; purchased from Sigma-Aldrich, Madrid, Spain) or AGN220675 (25 μM) added from more-concentrated solutions (prepared in serum-free medium and containing low amounts of DMSO) to obtain these final concentrations (final DMSO was always < 0.1%). Thirty min later, cells were exposed to malonate for 6 h, added from a solution prepared in a serum-free medium to obtain a final concentration of 40 mM in the wells. Control cells were maintained in the serum-free medium, but were not exposed to malonate or the different treatments. After malonate exposure, media from each well were used to measure lactate deshydrogenase (LDH) activity as an index of cell death, using the CytoTox 96 Non-Radioactive Cytotoxicity Assay Kit (G1780, Promega Biotech Ibérica, Madrid, Spain). In all experiments, the data of LDH activity were compared with the values obtained in a positive control with 1% Triton X-100 (Sigma-Aldrich, Madrid, Spain) that was taken as 100% of cell death. Compared with the Triton X-100-exposed cells, control cells (not exposed to malonate) accounted for a 10–20% of cell death, whereas malonate accounted for a 60–80%. For graphical presentation, the data in malonate-exposed cells (with or without the different additional treatments) were always expressed as the percentage over the data in the control cells (not exposed to malonate).

Analysis of endocannabinoid levels. Tissues or cells were homogenized in 5 volume of chloroform/methanol/Tris–HCl 50 mM (2 : 1 : 1) containing 10 pmol of d^8-anandamide, d^4-palmitoylethanolamide (PEA), d^4-oleylethanolamide (OEA) and d^5-2-AG. Deuterated standards were synthesized from d^8 arachidonic acid and ethanolamine or glycerol, or from d^4-ethanolamine and palmitic or oleic acid, as described ([53,54] respectively). Homogenates were centrifuged at 13 000 *g* for 16 min (4 °C), and the aqueous phase plus debris were collected and extracted again twice with 1 volume of chloroform. The organic phases from the three extractions were pooled and the organic solvents evaporated in a rotating evaporator. Lyophilized extracts were resuspended in chloroform/methanol 99 : 1 by volume. The solutions were then purified by open-bed chromatography on silica as described.[54] Fractions eluted with chloroform/methanol 9 : 1 by volume. (containing anandamide, 2-AG, OEA and PEA) were collected and the excess solvent evaporated with a rotating evaporator, and aliquots were analysed by isotope dilution liquid chromatography/atmospheric pressure chemical ionization/mass spectrometry (LC-APCI–MS) carried out under conditions described previously,[55] and allowing the separations of 2-AG, anandamide, OEA and PEA. MS detection was carried out in the selected ion-monitoring mode using *m/z* values of 356 and 348 (molecular ion $+1$ for deuterated and undeuterated anandamide), 384.35 and 379.35 (molecular ion $+1$ for deuterated and undeuterated 2-AG), 304 and 300 (molecular ion $+1$ for deuterated and undeuterated PEA) and 330 and 326 (molecular ion $+1$ for deuterated and undeuterated OEA). The amounts of endocannabinoids and related *N*-acylethanolamines were expressed as pmols/mg of lipids extracted. An amount of 1 mg of extracted lipids corresponds to $\sim$0.010–0.015 g of wet tissue weight.

Method for the extraction, purification and quantification of PGE2-G. Tissues and cells were homogenized in 5 volume of acetone containing 25 pmol of d4-PGE_2-G (a kind gift by Dr. DF Woodward, Allergan, Irvine, CA, USA). Homogenates were centrifuged at 13 000 *g* for 5 min (4 °C), and the debris was extracted again four times with 1 volume of acetone. The organic phases from the five extractions were pooled and the organic solvents evaporated in a rotating evaporator. Lyophilized extracts were resuspended in chloroform/methanol 99 : 1 by volume. The solutions were then purified by open-bed chromatography on silica using a gradient elution of chloroform/methanol to separate different class of lipids. Fractions eluted with chloroform/methanol 7 : 3 by volume. (containing PGE_2-G) were collected and the excess solvent evaporated with a rotating evaporator, and aliquots were analyzed by Liquid Chromatography-Electrospray-Ion Trap-Time of Flight (LC-ESI-IT-ToF) mass spectrometry. An IT-ToF mass spectrometer (Shimadzu) was used in conjunction with an LC-20AB (Shimadzu). LC analysis was performed in the isocratic mode using a DiscoveryC18 column (15 cm $\times$ 2.1 mm, 5 μm) and methanol/water/acetic acid (53 : 47 : 0.05 by volume.) as mobile phase with a flow rate of 0.15 ml/min. Identification of PGE_2-G (retention time 22.5 min) was carried out using ESI ionization in the positive mode with nebulizing gas flow of 1.5 ml/min and a curved desolvation line temperature of 250 °C. PGE_2-G quantification was performed by isotope dilution by using *m/z* values of 453.2766 and 449.2515, corresponding to the sodium adduct of the molecular ion $(M+23)^+$ for deuterated and undeuterated PGE_2-G, respectively. The full recovery of PGE_2-G from tissue due to the analytical procedure reported above was 44.9 $\pm$ 9.1. The LC-ESI-IT-ToF method described here for the first time is specific and sensitive with a limit of detection (defined as the concentration at which the signal/noise ratio is greater than 3 : 1) of 25 fmol. Moreover, the ratio between the $(M+23)^+$ peak areas of undeuterated (0.025–20 pmol) *versus.* deuterated (1 pmol) PGE_2-G varied linearly with the amount of undeuterated PGE_2-G. The quantification limit of PGE_2-G was 50 fmol.[56]

HPLC determination. Brain coronal slices (around 500 μm thick) were made at the level of the striatum.[57] Subsequently, this structure was dissected and homogenized in 20–40 volumes of cold 150 mM potassium phosphate buffer, pH 6.8, and distributed into two aliquots, one to be used for the analysis of protein concentration.[58] The other aliquot was used for the measurement of GABA contents by HPLC coupled to electrochemical detection.[11] It was diluted (½) with 0.4 N perchloric acid containing 0.4 mM sodium disulphite, 0.90 mM EDTA and β-aminobutirate as internal standard. Afterwards, samples were centrifuged for 3 min (15000 g) and the supernatants subjected to a previous derivatization process with *o*-phthaldehide (OPA)-sulphite solution (14.9 mM OPA, 45.4 mM sodium sulphite and 4.5% ethanol in 327 mM borate buffer, pH 10.4; see details in 11), previous to their injection into the HPLC system. This consisted of the following elements. The pump was an isocratic Spectra-Physics 8810. The column was an RP-18 (Spherisorb ODS-2; 150 mm, 4.6 mm, 5 μm particle size; Waters, Massachusetts, USA). The mobile phase, previously filtered and degassed, consisted of 0.06 M sodium dihydrogen phosphate, 0.06 mM EDTA and 20-30% methanol (pH 4.4). The flow rate was 0.8 ml/min. The effluent was monitored with a Metrohm bioanalytical system amperometric detector using a glassy carbon electrode. The potential was 0.85V relative to an Ag/AgCl reference electrode with a sensitivity of 50 nA (approx. 2 ng *per* sample). The signal was recorded on a Spectra-Physics 4290 integrator. The results were obtained from the peaks and calculated by comparison with the area under the corresponding internal standard peak. Values were expressed as μg/mg of protein.

Histological analyses. Fixed brains were sliced (35 μm-thick sections) in a vibratome. Free-floating sections obtained from each brain were incubated with a monoclonal anti-GFAP-Cy3 conjugate antibody (1 : 500, Sigma-Aldrich, Madrid, Spain) 24 h at room temperature. Following extensive washing, the brain sections were mounted on glass slides using the Vectashield Mounting Medium (Vector Laboratories, Burlingame, USA). In addition, the Hoescht staining was used for nuclear counterstaining. Adjacent sections to those used in the immunohistochemical analysis were used for Nissl staining, which allowed for the

determination of the number of cells after the different treatments done. A Nikon Eclipse 90i confocal microscope and a Nikon DXM 1200F camera were used for observation and photography, and all image processing techniques were performed using ImageJ, the software developed and freely distributed by the US National Institutes of Health (Bethesda. MD, USA).

Real time qRT-PCR analysis. Total RNA was isolated from lesioned or non-lesioned rat striata, or from cultured cells, using the RNATidy reagent (AppliChem., Cheshire, CT, USA). The total amount of RNA extracted was quantitated by spectrometry at 260 nm, and its purity was evaluated by the ratio between the absorbance values at 260 and 280 nm, whereas its integrity was confirmed in agarose gels. After the removal of genomic DNA (to eliminate DNA contamination), single-stranded complementary DNA was synthesized from 1 μg of total RNA using a commerical kit (Rneasy Mini Quantitect Reverse Transcription, Qiagen, Izasa, Madrid, Spain). The reaction mixture was kept frozen at $-20\,^{\circ}$C until enzymatic amplification. Quantitative real-time PCR assays were performed using TaqMan Gene Expression Assays (Applied Biosystems, Foster City, CA, USA) to quantify mRNA levels for COX-2 (reference: Rn01483828_m1), BDNF (reference: Rn01484928_m1), iNOS (reference: Rn00561646_m1), PPAR-α (reference: Rn00566193_m1), PPAR-γ (reference: Rn00440945_m1), MAGL (reference: Rn00593297_m1) and FAAH (reference: Rn00577086_m1), using β-actin expression (reference: Rn00667869_m1) as an endogenous control gene for normalization. The PCR assay was performed using the 7300 Fast Real-Time PCR System (Applied Biosystems, Foster City, CA, USA), and the threshold cycle (Ct) was calculated by the instrument's software (7300 Fast System, Applied Biosystems, Foster City, CA, USA).

Enzyme assays. 2-AG and anandamide hydrolysing activities were measured in cells after malonate treatment as described above for PGE_2-G measurement. In particular, 2-AG hydrolysis, which is mostly accounted for at least 80% by MAGL in neurons,[59] was measured by incubating the 10 000 *g* cytosolic fraction (70–100 μg/sample) of cells in Tris-HCl 50 mM, at pH 7.0 at 37 $^{\circ}$C for 20 min, with synthetic 2-arachidonoyl-(^{3}H)-glycerol (40 Ci/mmol, ARC St. Louis, MO, USA) properly diluted with 2-AG (Cayman Chemicals, Ann Arbor, MI, USA) to the final concentration of 50 μM. After incubation, the amount of [^{3}H]-glycerol produced was measured by scintillation counting of the aqueous phase after extraction of the incubation mixture with 2 volumes of $CHCl_3/CH_3OH$ 1 : 1 (by volume). Anandamide hydrolysis, which is almost uniquely accounted for FAAH in neurons, was measured by incubating the 10 000 *g* membrane fraction (70–100 μg/sample) of tissues in Tris-HCl 50 mM, at pH 9.0–10.00 at 37 $^{\circ}$C for 30 min, with synthetic *N*-arachidonoyl-[^{14}C]-ethanolamine (55 mCi/mmol, ARC St. Louis, MO, USA) properly diluted with anandamide (Tocris Bioscience, Avonmouth, Bristol, UK) to the final concentration of 10 μM. After incubation, the amount of [^{14}C]-ethanolamine produced was measured by scintillation counting of the aqueous phase after extraction of the incubation mixture with 2 volumes of $CHCl_3/CH_3OH$ 1 : 1 (by volume). In both cases, values were expressed as pmol of product formed/mg of protein in 1 minute of incubation.

Western blot analysis. Cultured cells (approximately 10^6/sample), exposed or not to 40 mM malonate for 6 h, were collected and washed twice in cold PBS and lysed on ice using the RIPA lysis solution. Lysates were maintained in ice for 20 min before a centrifugation of 15 min at 15 000 *g*. Supernatants were recovered and quantified by Bio-Rad DC Protein Assay Kit (Bio-Rad, Segrate, MI, Italy). Subsequently, 40–50 μg of lysates were boiled for 5 min in the Laemmli SDS loading buffer and loaded on precast polyacrylamide gels (4–12% gradient; Bolt Bis-Tris Plus gels; Life Technologies, Milan, Italy) and then transferred to a PVDF membrane. Filters were incubated overnight at 4 $^{\circ}$C with the following antibodies: mouse anti-FAAH antibody (1 μg/ml; from Sigma-Aldrich Milan, Italy; batch number: 11011-4H8) or rabbit anti-MAGL (1 : 200; Cayman Chemical, Ann Abor MI, USA). An anti α-tubulin antibody (1 : 5000; Sigma-Aldrich Milan, Italy) was used to check for equal protein loading. Reactive bands were detected by chemiluminescence (ECL or ECL-plus; Biorad, Segrate, MI, Italy). Images were analysed on a ChemiDoc station with Quantityone software (Bio-Rad, Segrate, MI, Italy). Data were calculated as the ratio between the optical densities of the protein and α-tubulin, but they were normalized as a percentage over the control group for presentation.

Statistical analyses. All data were assessed by one-way ANOVA followed by the Student–Newman–Keuls test, or by the unpaired Student's *t*-test, as required, using the GraphPad software (version 4.0).

Conflict of Interest

All authors declare that they have no conflicts of interest.

Acknowledgements. This work was supported by grants from CIBERNED (CB06/05/0089), MICINN (SAF2009/11847) and CAM (S2011/BMD-2308) to SV, MRP, OS and JFR, and by NIH (grant nr. DA009789) to VDM. MRP was a predoctoral fellow supported by the 'Programa FPI-Ministerio de Ciencia e Innovación' and SV was supported by the Complutense University-Predoctoral Program. We are indebted to Yolanda García Movellán and Davide Castelluccio for technical and administrative assistance.

1. Pazos MR, Sagredo O, Fernández-Ruiz J. The endocannabinoid system in Huntington's disease. *Curr Pharm Des* 2008; **14**: 2317–2325.
2. Fernández-Ruiz J, Moreno-Martet M, Rodríguez-Cueto C, Palomo-Garo C, Gómez-Cañas M, Valdeolivas S *et al.* Prospects for cannabinoid therapies in basal ganglia disorders. *Br J Pharmacol* 2011; **163**: 1365–1378.
3. Sagredo O, Pazos MR, Valdeolivas S, Fernández-Ruiz J. Cannabinoids: novel medicines for the treatment of Huntington's disease. *Recent Pat CNS Drug Discov* 2012; **7**: 41–48.
4. Walker FO. Huntington's disease. *Lancet* 2007; **369**: 218–228.
5. Cattaneo E, Zuccato C, Tartari M. Normal huntingtin function: an alternative approach to Huntington's disease. *Nat Rev Neurosci* 2005; **6**: 919–930.
6. McMurray CT. Huntington's disease: new hope for therapeutics. *Trends Neurosci* 2001; **24**: S32–S38.
7. Wright BL, Barker RA. Established and emerging therapies for Huntington's disease. *Curr Mol Med* 2007; **7**: 579–587.
8. Burgunder JM. Translational research in Huntington's disease: opening up for disease modifying treatment. *Transl Neurodegener* 2013; **2**: 2.

9. Lastres-Becker I, Bizat N, Boyer F, Hantraye P, Fernández-Ruiz J, Brouillet E. Potential involvement of cannabinoid receptors in 3-nitropropionic acid toxicity in vivo. *Neuroreport* 2004; **15**: 2375–2379.
10. Pintor A, Tebano MT, Martire A, Grieco R, Galluzzo M, Scattoni ML *et al.* The cannabinoid receptor agonist WIN 55,212-2 attenuates the effects induced by quinolinic acid in the rat striatum. *Neuropharmacology* 2006; **51**: 1004–1012.
11. Sagredo O, González S, Aroyo I, Pazos MR, Benito C, Lastres-Becker I *et al.* Cannabinoid CB2 receptor agonists protect the striatum against malonate toxicity: Relevance for Huntington's disease. *Glia* 2009; **57**: 1154–1167.
12. Sagredo O, Pazos MR, Satta V, Ramos JA, Pertwee RG, Fernández-Ruiz J. Neuroprotective effects of phytocannabinoid-based medicines in experimental models of Huntington's disease. *J Neurosci Res* 2011; **89**: 1509–1518.
13. Sagredo O, Ramos JA, Decio A, Mechoulam R, Fernández-Ruiz J. Cannabidiol reduced the striatal atrophy caused by 3-nitropropionic acid in vivo by mechanisms independent of the activation of cannabinoid, vanilloid TRPV1 and adenosine A2A receptors. *Eur J Neurosci* 2007; **26**: 843–851.
14. Palazuelos J, Aguado T, Pazos MR, Julien B, Carrasco C, Resel E *et al.* Microglial CB2 cannabinoid receptors are neuroprotective in Huntington's disease excitotoxicity. *Brain* 2009; **132**: 3152–3164.
15. Blázquez C, Chiarlone A, Sagredo O, Aguado T, Pazos MR, Resel E *et al.* Loss of striatal type 1 cannabinoid receptors is a key pathogenic factor in Huntington's disease. *Brain* 2001; **134**: 119–136.
16. Valdeolivas S, Satta V, Pertwee RG, Fernández-Ruiz J, Sagredo O. Sativex-like combination of phytocannabinoids is neuroprotective in malonate-lesioned rats, an inflammatory model of Huntington's disease: role of CB1 and CB2 receptors. *ACS Chem Neurosci* 2012; **3**: 400–406.
17. De Yébenes J. Phase II-clinical trial on neuroprotection with cannabinoids in Huntington's disease (SAT-HD). EudraCT 2010-024227-24.
18. Bisogno T, Di Marzo V. Short- and long-term plasticity of the endocannabinoid system in neuropsychiatric and neurological disorders. *Pharmacol Res* 2007; **56**: 428–442.
19. Bisogno T, Martire A, Petrosino S, Popoli P, Di Marzo V. Symptom-related changes of endocannabinoid and palmitoylethanolamide levels in brain areas of R6/2 mice, a transgenic model of Huntington's disease. *Neurochem Int* 2008; **52**: 307–313.
20. Lastres-Becker I, Fezza F, Cebeira M, Bisogno T, Ramos JA, Milone A *et al.* Changes in endocannabinoid transmission in the basal ganglia in a rat model of Huntington's disease. *Neuroreport* 2001; **12**: 2125–2129.
21. Lastres-Becker I, de Miguel R, De Petrocellis L, Makriyannis A, Di Marzo V, Fernández-Ruiz J. Compounds acting at the endocannabinoid and/or endovanilloid systems reduce hyperkinesia in a rat model of Huntington's disease. *J Neurochem* 2003; **84**: 1097–1109.
22. Toulmond S, Tang K, Bureau Y, Ashdown H, Degen S, O'Donnell R *et al.* Neuroprotective effects of M826, a reversible caspase-3 inhibitor, in the rat malonate model of Huntington's disease. *Br J Pharmacol* 2004; **141**: 689–697.
23. Lastres-Becker I, Bizat N, Boyer F, Hantraye P, Brouillet E, Fernández-Ruiz J. Effects of cannabinoids in the rat model of Huntington's disease generated by an intrastriatal injection of malonate. *Neuroreport* 2003; **14**: 813–816.
24. Bisogno T, Howell F, Williams G, Minassi A, Cascio MG, Ligresti A *et al.* Cloning of the first sn1-DAG lipases points to the spatial and temporal regulation of endocannabinoid signaling in the brain. *J Cell Biol* 2003; **163**: 463–468.
25. Sang N, Zhang J, Chen C. COX-2 oxidative metabolite of endocannabinoid 2-AG enhances excitatory glutamatergic synaptic transmission and induces neurotoxicity. *J Neurochem* 2007; **102**: 1966–1977.
26. Giordano M, Takashima H, Herranz A, Poltorak M, Geller HM, Marone M *et al.* Immortalized GABAergic cell lines derived from rat striatum using a temperature-sensitive allele of the SV40 large T antigen. *Exp Neurol* 1993; **124**: 395–400.
27. Bisogno T, Cascio MG, Saha B, Mahadevan A, Urbani P, Minassi A *et al.* Development of the first potent and specific inhibitors of endocannabinoid biosynthesis. *Biochim Biophys Acta* 2006; **1761**: 205–212.
28. Mechoulam R, Shohami E. Endocannabinoids and traumatic brain injury. *Mol Neurobiol* 2007; **36**: 68–74.
29. Cardona AE, Pioro EP, Sasse ME, Kostenko V, Cardona SM, Dijkstra IM *et al.* Control of microglial neurotoxicity by the fractalkine receptor. *Nat Neurosci* 2006; **9**: 917–924.
30. Brown GC. Mechanisms of inflammatory neurodegeneration: iNOS and NADPH oxidase. *Biochem Soc Trans* 2007; **35**: 1119–1121.
31. Stahel PF, Smith WR, Bruchis J, Rabb CH. Peroxisome proliferator-activated receptors: 'key' regulators of neuroinflammation after traumatic brain injury. *PPAR Res* 2008; **2008**: 538141.
32. Ortar G, Bisogno T, Ligresti A, Morera E, Nalli M, Di Marzo V. Tetrahydrolipstatin analogues as modulators of endocannabinoid 2-arachidonoylglycerol metabolism. *J Med Chem* 2008; **51**: 6970–6979.
33. Long JZ, Li W, Booker L, Burston JJ, Kinsey SG, Schlosburg JE *et al.* Selective blockade of 2-arachidonoylglycerol hydrolysis produces cannabinoid behavioral effects. *Nat Chem Biol* 2009; **5**: 37–44.
34. Nomura DK, Morrison BE, Blankman JL, Long JZ, Kinsey SG, Marcondes MC *et al.* Endocannabinoid hydrolysis generates brain prostaglandins that promote neuroinflammation. *Science* 2011; **334**: 809–813.
35. Piro JR, Benjamin DI, Duerr JM, Pi Y, Gonzales C, Wood KM *et al.* A dysregulated endocannabinoid-eicosanoid network supports pathogenesis in a mouse model of Alzheimer's disease. *Cell Rep* 2012; **1**: 617–623.
36. Minghetti L. Cyclooxygenase-2 (COX-2) in inflammatory and degenerative brain diseases. *J Neuropathol Exp Neurol* 2004; **63**: 901–910.
37. Tzeng SF, Hsiao HY, Mak OT. Prostaglandins and cyclooxygenases in glial cells during brain inflammation. *Curr Drug Targets Inflamm Allergy* 2005; **4**: 335–340.
38. Yang H, Chen C. Cyclooxygenase-2 in synaptic signaling. *Curr Pharm Des* 2008; **14**: 1443–1451.
39. Woodward DF, Carling RW, Cornell CL, Fliri HG, Martos JL, Pettit SN *et al.* The pharmacology and therapeutic relevance of endocannabinoid derived cyclo-oxygenase (COX)-2 products. *Pharmacol Ther* 2008; **120**: 71–80.
40. Hu SS, Bradshaw HB, Chen JS, Tan B, Walker JM. Prostaglandin E2 glycerol ester, an endogenous COX-2 metabolite of 2-arachidonoylglycerol, induces hyperalgesia and modulates NFkappaB activity. *Br J Pharmacol* 2008; **153**: 1538–1549.
41. Kozak KR, Prusakiewicz JJ, Marnett LJ. Oxidative metabolism of endocannabinoids by COX-2. *Curr Pharm Des* 2004; **10**: 659–667.
42. Kreutz S, Koch M, Böttger C, Ghadban C, Korf HW, Dehghani F. 2-Arachidonoyl-glycerol elicits neuroprotective effects on excitotoxically lesioned dentate gyrus granule cells via abnormal-cannabidiol-sensitive receptors on microglial cells. *Glia* 2009; **57**: 286–294.
43. Sun Y, Bennett A. Cannabinoids: a new group of agonists of PPARs. *PPAR Res* 2007; **2007**: 23513.
44. Panikashvili D, Simeonidou C, Ben-Shabat S, Hanus L, Breuer A, Mechoulam R *et al.* An endogenous cannabinoid (2-AG) is neuroprotective after brain injury. *Nature* 2001; **413**: 527–531.
45. O'Sullivan SE, Kendall DA. Cannabinoid activation of peroxisome proliferator-activated receptors: potential for modulation of inflammatory disease. *Immunobiology* 2010; **215**: 611–616.
46. Minghetti L, Greco A, Potenza RL, Pezzola A, Blum D, Bantubungi K *et al.* Effects of the adenosine A2A receptor antagonist SCH 58621 on cyclooxygenase-2 expression, glial activation, and brain-derived neurotrophic factor availability in a rat model of striatal neurodegeneration. *J Neuropathol Exp Neurol* 2007; **66**: 363–371.
47. Teismann P, Tieu K, Choi DK, Wu DC, Naini A, Hunot S *et al.* Cyclooxygenase-2 is instrumental in Parkinson's disease neurodegeneration. *Proc Natl Acad Sci USA* 2003; **100**: 5473–5478.
48. Hoozemans JJ, Rozemuller JM, van Haastert ES, Veerhuis R, Cyclooxygenase-1 Eikelenboom P. and -2 in the different stages of Alzheimer's disease pathology. *Curr Pharm Des* 2008; **14**: 1419–1427.
49. Gopez JJ, Yue H, Vasudevan R, Malik AS, Fogelsanger LN, Lewis S *et al.* Cyclooxygenase-2-specific inhibitor improves functional outcomes, provides neuroprotection, and reduces inflammation in a rat model of traumatic brain injury. *Neurosurgery* 2005; **56**: 590–604.
50. Wang QJ. PKD at the crossroads of DAG and PKC signaling. *Trends Pharmacol Sci* 2006; **27**: 317–323.
51. Zhang J, Chen C. Endocannabinoid 2-arachidonoylglycerol protects neurons by limiting COX-2 elevation. *J Biol Chem* 2008; **283**: 22601–22611.
52. Du H, Chen X, Zhang J, Chen C. Inhibition of COX-2 expression by endocannabinoid 2-arachidonoylglycerol is mediated via PPAR-γ. *Br J Pharmacol* 2001; **163**: 1533–1549.
53. Devane WA, Hanus L, Breuer A, Pertwee RG, Stevenson LA, Griffin G *et al.* Isolation and structure of a brain constituent that binds to the cannabinoid receptor. *Science* 1992; **258**: 1946–1949.
54. Bisogno T, Sepe N, Melck D, Maurelli S, De Petrocellis L, Di Marzo V. Biosynthesis, release and degradation of the novel endogenous cannabimimetic metabolite 2-arachidonoylglycerol in mouse neuroblastoma cells. *Biochem J* 1997; **322**: 671–677.
55. Marsicano G, Wotjak CT, Azad SC, Bisogno T, Rammes G, Cascio MG *et al.* The endogenous cannabinoid system controls extinction of aversive memories. *Nature* 2002; **418**: 530–534.
56. Gatta L, Piscitelli F, Giordano C, Boccella S, Lichtman A, Maione S *et al.* Discovery of prostamide F2α and its role in inflammatory pain and dorsal horn nociceptive neuron hyperexcitability. *PLoS One* 2012; **7**: e31111.
57. Palkovits M, Brownstein J. *Maps and Guide to Microdissection of the Rat Brain*. Elsevier: New York-Amsterdam-London, 1988.
58. Lowry OH, Rosebrough NJ, Farr AL, Randall RJ. Protein measurement with the Folin phenol reagent. *J Biol Chem* 1951; **193**: 265–275.
59. Blankman JL, Simon GM, Cravatt BF. A comprehensive profile of brain enzymes that hydrolyze the endocannabinoid 2-arachidonoylglycerol. *Chem Biol* 2007; **14**: 1347–1356.